View Article Online / Journal Homepage / Table of Contents for this issue
Dynamic Article Links

Catalysis
Science & Technology

Cite this: *Catal. Sci. Technol.*, 2011, **1**, 638–643

www.rsc.org/catalysis

PAPER

Low-temperature hydrogenation of the C=O bond of propanal over Ni–Pt bimetallic catalysts: from model surfaces to supported catalysts

Renyang Zheng,[a] Michael P. Humbert,[b] Yuexiang Zhu*[a] and Jingguang G. Chen*[b]

Received 1st March 2011, Accepted 4th April 2011
DOI: 10.1039/c1cy00066g

Published on 28 April 2011. Downloaded on 22/01/2016 00:55:10.

The hydrogenation of propanal is used as a probe reaction to correlate the activity of C=O bond hydrogenation over Ni–Pt bimetallic surfaces and catalysts. Density functional theory (DFT) calculations predict that propanal is more weakly bonded on the Pt–Ni–Pt(111) subsurface structure than on either Ni or Pt, suggesting a possible novel low-temperature hydrogenation pathway based on a previous trend predicted for C=C hydrogenation. Surface science studies using temperature programmed desorption (TPD) on Ni-modified polycrystalline Pt foil verify that different bimetallic surface structures exhibit distinct C=O hydrogenation activity, with the Pt–Ni–Pt subsurface structure being much more active for propanal hydrogenation. Furthermore, γ-Al_2O_3 supported Ni–Pt bimetallic catalysts have been prepared to extend the surface science studies to real world catalysis. In the gas phase hydrogenation of propanal, both batch and flow reactor studies show that Ni–Pt/γ-Al_2O_3 bimetallic catalysts exhibit enhanced C=O hydrogenation activity compared to the corresponding monometallic catalysts. The excellent correlation between theoretical predictions, surface science studies on model surfaces, and catalytic evaluation of supported catalysts demonstrates the feasibility to rationally design bimetallic catalysts with enhanced hydrogenation activity.

1. Introduction

Bimetallic catalysts often show electronic and chemical properties that differ distinctly from those of the parent metals.[1–4] Many investigations have demonstrated that combined surface science studies and theoretical calculations on single crystal surfaces can be used to understand and predict the catalytic properties of bimetallic catalysts.[5–8] In bimetallic systems consisting of one monolayer of an admetal deposited on a single crystal substrate of another metal, the admetal can occupy the topmost surface sites to produce the surface monolayer structure, diffuse into the subsurface region to form the subsurface monolayer configuration, or alloy with the substrate surface to produce intermixed bimetallic surfaces.[4] It has been demonstrated that a Pt-terminated Pt–Ni–Pt(111) subsurface bimetallic structure showed much higher activity for the hydrogenation of cyclohexene than a Ni-terminated Ni–Pt–Pt(111) surface and the corresponding monometallic Pt(111) and Ni(111) surfaces.[7] The novel low temperature hydrogenation pathway on the subsurface bimetallic structures has been correlated to the presence of weakly bonded atomic hydrogen and cyclohexene, due to the modification of the electronic properties of Pt by the subsurface Ni atoms.[7] More recently, the surface science results were extended to γ-Al_2O_3 supported Ni–Pt and Co–Pt bimetallic and the corresponding monometallic catalysts.[9,10] The trend observed in the catalytic activity of cyclohexene hydrogenation at a relatively low temperature, 303 K, is identical to that predicted from single crystal surfaces: Ni–Pt > Co–Pt > Pt.[7] The novel low temperature hydrogenation over a γ-Al_2O_3 supported Ni–Pt bimetallic catalyst was also carried out in conjugated hydrocarbon molecules, such as benzene and 1,3-butadiene.[9,11] These results reveal that Ni–Pt/γ-Al_2O_3 is more active than Ni or Pt for C=C bond hydrogenation.

The main objectives of the present work are twofold. First, to explore whether the Ni–Pt bimetallic catalyst would show enhanced activity for C=O bond hydrogenation. Second, to investigate whether predictions from DFT calculations and surface science experiments would be verified in supported catalysts. Here we select propanal as the probe molecule to answer these questions using three parallel approaches: (1) DFT calculations of the binding energy of propanal; (2) fundamental surface science studies using temperature programmed desorption (TPD) of propanal hydrogenation on model surfaces; (3) synthesis and catalytic evaluation of γ-Al_2O_3 supported catalysts. For gas phase hydrogenation of

[a] *Beijing National Laboratory for Molecular Sciences, State Key Laboratory for Structural Chemistry of Unstable and Stable Species, College of Chemistry and Molecular Engineering, Peking University, Beijing 100871, China. E-mail: zhuyx@pku.edu.cn*
[b] *Department of Chemical Engineering, Center for Catalytic Science and Technology, University of Delaware, Newark, DE 19716, USA. E-mail: jgchen@udel.edu*

This journal is © The Royal Society of Chemistry 2011

View Article Online

Published on 28 April 2011. Downloaded on 22/01/2016 00:55:10.

propanal, batch reactor studies using Fourier transform infrared spectroscopy (FTIR) are employed to quantify the rate constants for hydrogenation, while flow reactor studies using gas chromatography (GC) are performed to obtain the steady-state conversion and activation barriers.

Catalytic hydrogenation of the C=O bond is an important industrial reaction for organic synthesis.[12,13] Catalysts based on transition metals, such as Pt,[14] Pd,[15] Rh,[16] and Ni–Mo,[17] have been reported for the hydrogenation of propanal to produce 1-propanol. Additionally, studies of the hydrogenation of propanal, which is a possible product of the hydrogenation of acrolein, may provide information on the selective hydrogenation of the C=O bond in α,β-unsaturated aldehydes.[18–20] More recently, C=O bond hydrogenation has been considered as an important initial step in catalytic conversion of cellulosic biomass.[21,22] Therefore, understanding the relationship between the catalyst formulation and catalytic property for propanal hydrogenation should also provide useful information on the selection of catalysts for the hydrogenation of unsaturated aldehydes and the catalytic conversion of cellulose.

2. Theoretical and experimental methods

2.1 DFT calculations

The binding energies of propanal were calculated using the periodic density functional theory as implemented in the Vienna Ab-initio Simulations Package (VASP) code.[23,24] The standard calculation procedure can be found in a recent review.[4] A plane wave cutoff energy of 396 eV was used for all calculations using the PW91 functional. A periodic 3 × 3 unit cell structure was modeled using four layers of metal separated by six equivalent layers of vacuum. For the four layers of metal, the bottom two layers were frozen at the bulk Pt–Pt distance of 2.83 Å, while the top two layers were allowed to relax to reach the lowest energy configuration. Propanal was placed onto the surface in the perpendicular ($\eta_1\mu_1$) adsorption mode, which was found to be the most stable configuration reported in the literature,[25] with an initial adsorbate-surface bond distance of 2 Å. The surface d-band center value was calculated as the first order moment of the projected d-band density of states on the surface atoms with respect to the Fermi level.

2.2 TPD measurements

The ultrahigh vacuum (UHV) chamber used for the TPD study was a two-level stainless steel system with a base pressure of 1×10^{-10} Torr, as described elsewhere.[7,26] The chamber was equipped with a quadrupole mass spectrometer (QMS) for TPD experiments and for *in situ* verification of reagent purity. The TPD of propanal hydrogenation was performed on a polycrystalline Pt foil. The Pt foil was spot welded to two tantalum posts used as electrical and thermal contacts for resistive heating and liquid nitrogen cooling. The Pt foil temperature was measured and controlled from 100 K to 1100 K *via* a K-type thermocouple. To prepare a clean Pt surface, the Pt foil was first subjected to Ne^+ sputtering at approximately 600 K. The surfaces were then exposed to oxygen at elevated temperatures (~890 K) to remove any excess carbon followed by annealing at 1100 K. The surface cleanliness was verified with Auger electron spectroscopy (AES).

To prepare the Ni-modified Pt foil, Ni was deposited onto the clean Pt foil at 300 K until the AES peak-to-peak ratio of Ni (849 eV)/Pt (241 eV) was approximately 1.7. This ratio corresponds to about one monolayer (ML) of Ni residing on top of the Pt as estimated by standard substrate/overlayer calculations,[27] under the assumption that Ni grows on Pt in a layer-by-layer manner. This surface is designated as Ni–Pt–Pt. The surface monolayer Ni could then be driven into the subsurface region by flashing the Ni–Pt–Pt surface to 723 K and holding for 30 s.[27] This resulted in the Ni (849 eV)/Pt (241 eV) AES ratio decreasing to 1.0, representative of a Pt surface with most of the Ni present in the subsurface region. This structure is designated as the Pt–Ni–Pt subsurface structure. Additionally, a thick Ni surface was made by depositing 5 ML of Ni onto Pt foil at 300 K.

After the bimetallic surfaces were synthesized, hydrogen and propanal were dosed to the surfaces with an exposure of 1 L (1 L = 1×10^{-6} Torr s) and 5 L, respectively. The propanal was purified by successive freeze–pump–thaw cycles before use. The TPD experiments were performed with a linear heating rate of 3 K s^{-1}.

2.3 Preparation and characterization of supported catalysts

The γ-Al_2O_3 supported catalysts were prepared by a slurry-based impregnation method. The $Ni(NO_3)_2{\cdot}6H_2O$ and $Pt(NH_3)_4(NO_3)_2$ (Alfa Aesar) precursors were dissolved in an excess of deionized water (15 mL H_2O per gram of the catalyst) and then impregnated into the γ-Al_2O_3 (Alfa Aesar, Product Number of 39812). The solution was sonicated for 1 h, then dried at 373 K for 24 h, and finally calcined at 563 K for 2 h to produce the 5.0 wt% Ni–1.7 wt% Pt/γ-Al_2O_3 and 1.5 wt% Ni–1.7 wt% Pt/γ-Al_2O_3 bimetallic catalysts, with a Ni : Pt metal atomic ratio of 10 : 1 and 3 : 1, respectively. The corresponding monometallic Ni and Pt catalysts were also prepared to serve as control samples.

Pulse CO chemisorption was performed using an Altamira Instruments AMI-200ip to measure the number of active sites on the surfaces of the reduced catalysts. Approximately 0.1 g of the catalyst was reduced by H_2 at 723 K for 2 h and then cooled in He. After cooling, pulses of CO in a He carrier (CO/He molar ratio = 1 : 1) were injected at 20 mL min^{-1} at room temperature and the signal was monitored by a thermal conductivity detector (TCD).

2.4 Catalytic evaluation of supported catalysts

2.4.1 Batch reactor studies using FTIR. Fourier transform infrared spectroscopy (FTIR) was used to monitor the concentrations of individual reactants and products during hydrogenation reactions within a batch reactor system that is based on a design reported elsewhere in the literature.[11,28] In brief, it is a stainless steel IR cell fitted with BaF_2 windows with a base pressure below 1×10^{-6} Torr. This design allowed *in situ* reduction of samples and spectroscopic measurements of either surface species or gas-phase molecules before, during, and after reduction/reaction. All FTIR spectra were recorded

View Article Online

Published on 28 April 2011. Downloaded on 22/01/2016 00:55:10.

with 4 cm^{-1} resolution using a Nicolet-470 FTIR spectrometer equipped with a MCT-A (mercury cadmium telluride) detector.

Powder catalyst samples of 25 mg were pressed onto a square tungsten mesh, which had a K-type thermocouple affixed *via* spot-welding to monitor the catalyst temperature. To remove water and other impurities the cell was evacuated to a pressure below 10^{-6} Torr at room temperature. The catalyst was then reduced at 723 K in 30 Torr H_2 for 10 min followed by evacuation and a high temperature flash (723 K) to remove any surface species generated during the reduction. The reduction cycle was repeated three times before performing hydrogenation experiments. The gas-phase reactants and products were monitored by recording FTIR spectra every 30 s during the reaction. In order to obtain comparable reaction rates between samples with different metal loadings, the propanal hydrogenation over 5.0 wt% Ni–1.7 wt% Pt/γ-Al_2O_3 was performed at 308 K with a hydrogen to propanal ratio of 2 : 1, while that over 1.5 wt% Ni–1.7 wt% Pt/γ-Al_2O_3 was performed at 343 K with the hydrogen to propanal ratio of 4 : 1. The concentrations of propanal and 1-propanol were determined using the peak areas of the characteristic ν(C=O) mode at 1744 cm^{-1} and the ν(O–H) mode at 3670 cm^{-1}, respectively. The concentration was calibrated by measuring the vibrational intensity of each compound at various gas-phase pressures in a range relevant to the current study.

2.4.2 Flow reactor studies using gas chromatography (GC). The vapor phase hydrogenation of propanal was also carried out by flow reactor studies in a quartz glass reactor under atmospheric pressure at 308 K. Prior to reaction, 0.10 g of the catalyst was reduced in a H_2 (20 mL min^{-1}) and N_2 (20 mL min^{-1}) mixture at 723 K for 1 h. The catalysts were completely reduced by the reduction process.[9,11] During the reaction, the flow of propanal, controlled by a micro-syringe pump with a liquid flow rate of 0.5 mL h^{-1}, was carried by a H_2 (20 mL min^{-1}) and N_2 (20 mL min^{-1}) mixture. The ratio of H_2 to propanal was calculated to be 8 : 1. The products were analyzed by using an online GC equipped with a flame ionization detector (FID). The apparent activation barriers (E_a) for propanal hydrogenation were estimated by performing flow reactor studies over these catalysts at different temperatures between 308 and 418 K, with the conversion between 1% and 15%. Prior to the E_a measurement, the catalyst was left on stream for at least 300 min to achieve a relatively stable conversion.

3. Results and discussion

3.1 DFT calculations of propanal binding energies

In previous studies the enhanced C=C bond hydrogenation activity of cyclohexene has been correlated with the presence of weakly bonded cyclohexene on several Pt-based bimetallic catalysts.[7] To determine whether such a correlation can be extended to C=O bond hydrogenation, DFT calculations were performed in the current study and the results are summarized in Table 1. The value of the surface d-band center has been found to be a useful descriptor to correlate the binding strength of many adsorbates on the bimetallic surfaces.[4] In general, the binding energies of propanal increase as the surface d-band center moves closer to the Fermi level, with binding energies being the weakest on the Pt–Ni–Pt(111) subsurface structure. The binding energy of propanal on these surfaces follows the trend of Pt–Ni–Pt(111) < Pt(111) < Ni(111) < Ni–Pt–Pt(111), identical to that of alkenes on these surfaces.

Table 1 Summary of DFT calculations of d-band center values and binding energies of propanal based on the Pt(111) substrate, and normalized 1-propanol yield based on Pt foil from TPD experiments

Surfaces	d-Band center/eV	Binding energy of propanal/kJ mol^{-1}	Normalized 1-propanol yield
Pt–Ni–Pt	−2.74	−12.5	1.00
Pt	−2.58	−15.0	0.05
Ni	−1.48	−28.9	0
Ni–Pt–Pt	−1.19	−74.1	0.08

3.2 TPD results

The DFT results in Table 1 predict that propanal should be more weakly bonded on the Pt–Ni–Pt(111) subsurface structure than the corresponding monometallic surfaces, suggesting that Pt–Ni–Pt(111) should be more active toward propanal hydrogenation. The prediction is confirmed experimentally in Fig. 1 by comparing the TPD results of propanal hydrogenation activity on polycrystalline Pt, Ni–Pt–Pt, Pt–Ni–Pt, and a thick Ni-modified Pt surface.

In the current study a polycrystalline Pt foil was used to prepare the monometallic and bimetallic model surfaces. Results from previous studies indicated that both the (111) and (100) facets are present on the Pt foil,[26,29] and that the Pt foil showed general similarities in the activity and stability to those of single crystal Pt(111).[26] Comparing to Pt(111), the utilization of a polycrystalline Pt foil should provide a more realistic model surface to represent the complex morphology of supported catalysts.

Fig. 1 displays the masses characteristic of the hydrogenation product, 1-propanol (CH_3–CH_2–CH_2–OH, 31 amu), and molecularly desorbed propanal (CH_3–CH_2–CH=O, 58 amu).[30] The peaks at 127 and 177 K in the mass 31 amu spectra are from the cracking patterns of molecularly desorbed propanal based on the similar peak shape and desorption temperature between the 31 and 58 amu spectra. The production of 1-propanol is detected

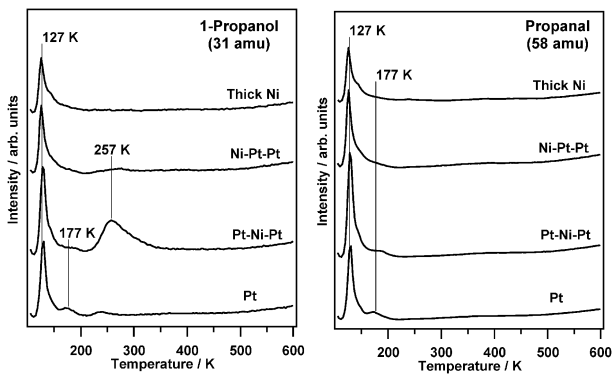

Fig. 1 TPD spectra of propanal hydrogenation on Ni-modified polycrystalline Pt foil.

This journal is © The Royal Society of Chemistry 2011

View Article Online

Published on 28 April 2011. Downloaded on 22/01/2016 00:55:10.

from the subsurface Pt–Ni–Pt at 257 K. In comparison, there is only a small peak around 257 K from either the Ni–Pt–Pt or Pt foil surfaces, and no peak from the thick Ni foil surfaces. The relative yields of 1-propanol from the four surfaces are quantified from the TPD peak areas and also shown in Table 1. The Pt–Ni–Pt subsurface structure is much more active toward propanal hydrogenation than the other three surfaces. By comparing the trends in the DFT and TPD results in Table 1, it indicates that the higher hydrogenation activity on Pt–Ni–Pt is related to the weaker binding energies of propanal, in agreement with the trend observed previously for the C=C bond hydrogenation.[10]

3.3 Characterization and reactor evaluation of supported catalysts

The γ-Al_2O_3 supported catalysts were synthesized to extend the fundamental surface science studies and theoretical predictions to the real world catalysis. The CO uptake values of 1.5 wt%Ni–1.7 wt%Pt/γ-Al_2O_3, 5.0 wt%Ni–1.7 wt%Pt/γ-Al_2O_3 and the monometallic catalysts are listed in Table 2. It shows that both Ni and Pt monometallic catalysts adsorb CO at room temperature. The Ni–Pt/γ-Al_2O_3 bimetallic catalysts have larger CO uptake values than Pt/γ-Al_2O_3 due to the presence of additional adsorption sites of Ni metal atoms, with the CO uptake value increasing as the amount of Ni in the catalyst increases. The amount of adsorbed CO per gram of the catalyst provides a quantitative description of the number of active sites, which is used to normalize the reaction rate constants derived from the batch reactor measurements.

The monometallic and bimetallic catalysts used in the current study have been characterized previously using Transmission Electron Microscopy (TEM) and Extended X-ray Absorption Structure (EXAFS).[11] The TEM results revealed that all catalysts contained relatively uniform metal particles approximately 2 nm in size. The EXAFS characterization confirmed the formation of the Ni–Pt bonds in both bimetallic catalysts.

A batch reactor was employed to evaluate the rate of C=O bond hydrogenation of propanal. Fig. 2 displays the consumption of propanal and production of 1-propanol as a function of reaction time for the bimetallic and corresponding monometallic catalysts. The sum of the gas-phase concentrations of propanal and 1-propanol is constant during the reaction time of 3 h, indicating that 1-propanol is the only hydrogenation product. Fig. 2(A) clearly shows the production of 1-propanol

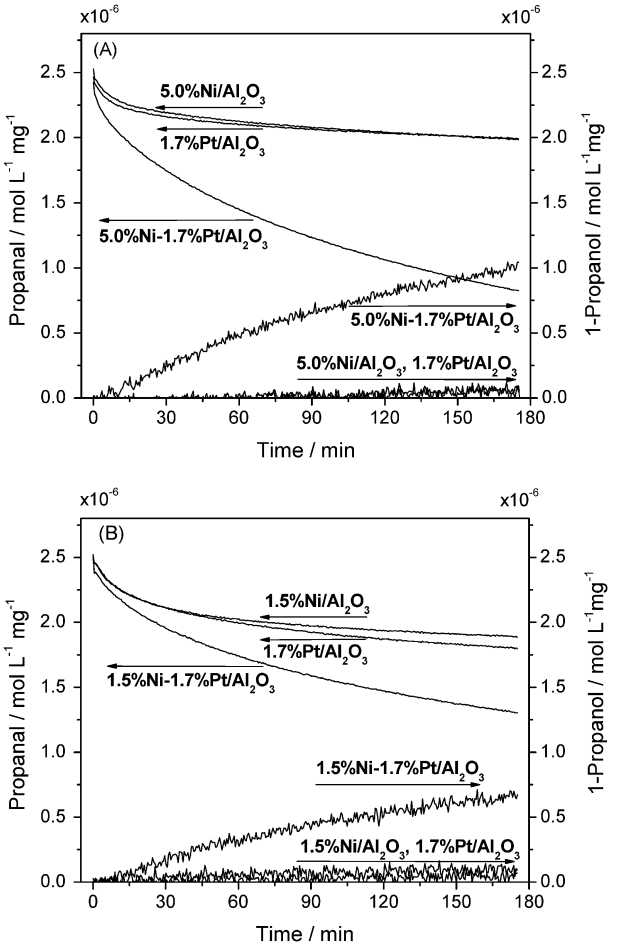

Fig. 2 Batch reactor results of propanal hydrogenation: (A) 5.0 wt% Ni–1.7 wt% Pt/γ-Al_2O_3 series of catalysts at 308 K with a feed ratio of H_2/propanal = 2 : 1 and (B) 1.5 wt% Ni–1.7 wt% Pt/γ-Al_2O_3 series of catalysts at 343 K with a feed ratio of H_2/propanal = 4 : 1.

over the 5.0 wt% Ni–1.7 wt% Pt/γ-Al_2O_3 bimetallic catalyst, whereas only a trace amount of 1-propanol is produced over the monometallic Ni and Pt catalysts. In this set of experiments, a H_2/propanal feed ratio of 2 : 1 and a reaction temperature of 308 K were used. Under the same reaction conditions, however, the 1.5 wt% Ni–1.7 wt% Pt/γ-Al_2O_3 is much less active than 5.0 wt% Ni–1.7 wt%Pt/γ-Al_2O_3 (data not shown here). To obtain comparable reaction rates, the reaction temperature was raised to 343 K and the feed

Table 2 Catalyst compositions, CO chemisorption results, reaction rate constants from batch reactor studies, and apparent activation barriers from flow reactor studies of propanal hydrogenation

Catalyst	CO uptake/μmol g^{-1}	$k/10^{-3}$ min^{-1} g^{-1}	$k^{rc}/10^{-3}$ min^{-1} μmol CO^{-1}	E_a/kJ mol^{-1}
1.7 wt%Pt/γ-Al_2O_3[a]	38.9	15	0.39	53.0
5.0 wt%Ni/γ-Al_2O_3[a]	55.8	20	0.35	37.3
5.0 wt%Ni–1.7 wt%Pt/γ-Al_2O_3[a]	97.0	230	2.37	25.9
1.7 wt%Pt/γ-Al_2O_3[b]	—	28	0.71	—
1.5 wt%Ni/γ-Al_2O_3[b]	28.8	18	0.61	45.7
1.5 wt%Ni–1.7 wt%Pt/γ-Al_2O_3[b]	49.2	137	2.78	24.4

[a] Batch reactor reaction conditions of 5.0 wt%Ni–1.7 wt%Pt/γ-Al_2O_3 series of catalysts: H_2/propanal = 2 : 1, T = 308 K, catalyst amount: 25 mg. [b] Batch reactor reaction conditions of 1.5 wt%Ni–1.7 wt%Pt/γ-Al_2O_3 series of catalysts: H_2/propanal = 4 : 1, T = 343 K, catalyst amount: 25 mg. [c] Normalized rate constants by CO chemisorption results.

View Article Online

Published on 28 April 2011. Downloaded on 22/01/2016 00:55:10.

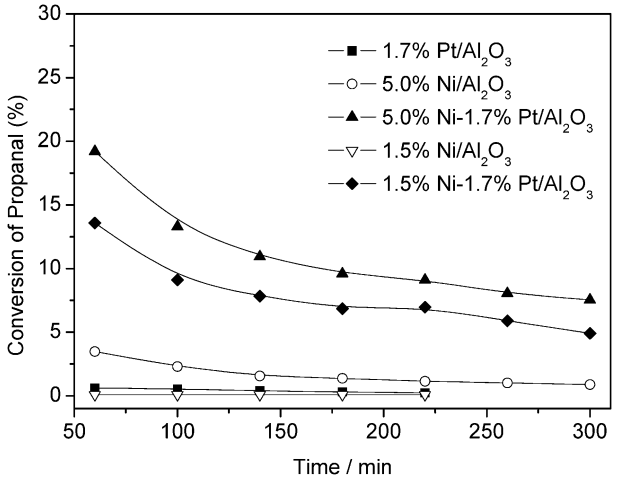

Fig. 3 Flow reactor results of propanal hydrogenation at 308 K. Reaction conditions: H_2 : propanal = 8 : 1, catalyst amount: 100 mg.

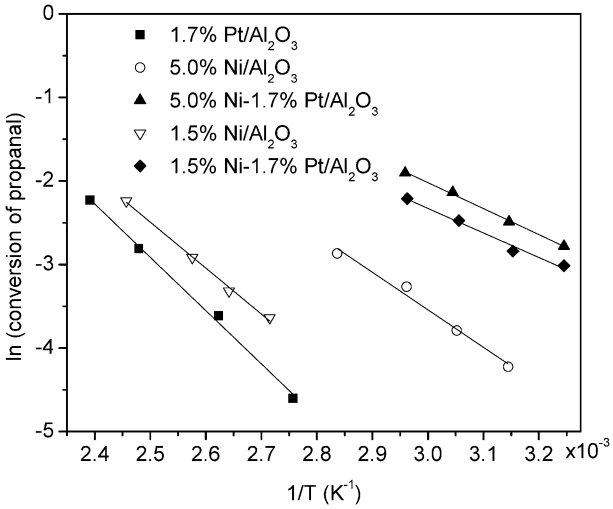

Fig. 4 Estimation of the apparent activation energy for propanal hydrogenation from flow reactor studies.

ratio of H_2/propanal was also increased to 4 : 1, as shown in Fig. 2(B). Similar to the 5.0 wt% Ni–1.7 wt% Pt/γ-Al_2O_3 series catalysts, the consumption of propanal and production of 1-propanol over the 1.5 wt% Ni–1.7 wt %Pt/γ-Al_2O_3 bimetallic catalyst are much faster than those over the monometallic Ni and Pt catalysts. To make a quantitative comparison, the C═O bond hydrogenation rate is estimated by fitting a first order rate equation for the consumption of propanal, as listed in Table 2. The rate constant is also normalized to the CO uptake of each catalyst obtained from the CO chemisorption measurements.

The conversion of propanal obtained from a flow reactor is presented in Fig. 3. The only reaction product detected by the online GC after 1 h of reaction is 1-propanol. Fig. 3 shows that the trend in conversion is 5.0 wt% Ni–1.7 wt% Pt/γ-Al_2O_3 > 1.5 wt% Ni–1.7 wt% Pt/γ-Al_2O_3 ≫ 5.0 wt% Ni/γ-Al_2O_3 > 1.7 wt% Pt/γ-Al_2O_3 > 1.5 wt %Ni/γ-Al_2O_3, suggesting once again that Ni–Pt bimetallic catalysts exhibit higher C═O bond hydrogenation activity than the monometallic Ni and Pt catalysts, in agreement with the trend observed in the batch reactor studies. This observation is consistent with our previous studies of butanal hydrogenation,[31] where monolayer dispersed Pt/Ni bimetallic particles possess higher hydrogenation activity.

Additionally, the apparent activation barriers (E_a) for propanal hydrogenation were estimated by performing catalytic studies at different temperatures, as shown in the Arrhenius plots in Fig. 4. The values are compared in Table 2. Both Ni–Pt bimetallic catalysts exhibit the lowest E_a values of approximately 25 kJ mol^{-1}, with the trend of Ni–Pt < Ni < Pt. The lower E_a value is consistent with the observation of low-temperature C═O bond hydrogenation activity over the Ni–Pt bimetallic surfaces (Fig. 1) and catalysts (Fig. 2 and 3).

3.4 Correlating reactor studies with DFT calculations and surface science results

In previous studies of the hydrogenation of alkenes, one hypothesis for promoting the low-temperature hydrogenation of the C═C bond is that the atomic hydrogen and alkenes should bond relatively weakly on the catalyst to facilitate the hydrogenation process.[10] Furthermore, a volcano-type relationship has been identified between binding energy and hydrogenation activity for cyclohexene over several Pt-based bimetallic surfaces,[7] with the subsurface Pt–Ni–Pt structure being identified as having an optimal cyclohexene binding energy for hydrogenation. Using the same binding energy argument, one would predict that the weaker binding energy of propanal on Pt–Ni–Pt(111) should lead to a higher C═O hydrogenation activity than that on either Ni–Pt–Pt(111) or the corresponding monometallic surfaces. This hypothesis is confirmed in the TPD results on Ni-modified Pt foil, with the subsurface Pt–Ni–Pt structure being much more active than the other surfaces for propanal hydrogenation.

Batch and flow reactor studies of propanal hydrogenation on Ni–Pt/γ-Al_2O_3 catalysts present an effort to bridge the "materials gap" and "pressure gap" between surface science studies under ultrahigh vacuum conditions and reactor evaluation of supported catalysts under catalytic conditions. The results show that Ni–Pt/γ-Al_2O_3 catalysts exhibit significantly higher C═O hydrogenation activity than the corresponding monometallic catalysts. Previous studies on supported bimetallic catalysts by FTIR spectroscopy of adsorbed carbon monoxide have shown that the surfaces of the Ni–Pt catalysts are composed of primarily Pt atoms,[11] suggesting that the nanoparticle structure may more closely resemble the Pt-terminated subsurface configuration than the Ni-terminated surface structure. Moreover, recent DFT calculations[32] and experimental verification[33] show that the subsurface Pt–Ni–Pt structure is preferred thermodynamically over Ni–Pt–Pt in the presence of adsorbed hydrogen. Therefore, one can conclude that the enhanced propanal hydrogenation activity observed over supported Ni–Pt/γ-Al_2O_3 could be due to the presence of Pt-terminated structures, similar to the Pt–Ni–Pt configuration identified in surface science and theoretical calculations. Overall, the results in the current study demonstrate excellent agreement in the trends in propanal binding energy from DFT calculations, 1-propanol yield from TPD studies on polycrystalline Pt foil,

 This journal is © The Royal Society of Chemistry 2011

View Article Online

Published on 28 April 2011. Downloaded on 22/01/2016 00:55:10.

and catalytic evaluation over supported catalysts from batch and flow reactor studies. More importantly, the correlation of the binding energy with the surface d-band center provides the possibility to predict other desirable bimetallic formulations and structures for the C═O hydrogenation, based on the large database of d-band center values for a wide range of bimetallic systems.[4] More detailed catalyst characterization and reactor studies, such as the hydrogenation of unsaturated aldehydes, are needed to further validate the unique hydrogenation activity of the Ni–Pt bimetallic catalysts.

4. Conclusions

The feasibility of predicting desirable bimetallic catalysts by DFT calculations and surface science experiments has been investigated using propanal hydrogenation as a probe reaction. DFT calculations are performed to predict the weaker binding energies of propanal on the subsurface Pt–Ni–Pt(111) structure. TPD results on Ni-modified polycrystalline Pt foil verify that the subsurface Pt–Ni–Pt structure exhibits higher C═O bond hydrogenation activity than the surface Ni–Pt–Pt structure and the monometallic Ni and Pt surfaces. To bridge the "materials gap" and "pressure gap" between fundamental surface science studies and real world catalysis, γ-Al_2O_3 supported Ni–Pt bimetallic catalysts with a Ni/Pt molar ratio of 3 : 1 and 10 : 1 are evaluated using batch and flow reactors, which confirm that the Ni–Pt/γ-Al_2O_3 catalysts exhibit significantly higher propanal hydrogenation activity than the corresponding monometallic catalysts. The enhanced hydrogenation activity observed over the Ni–Pt/γ-Al_2O_3 catalysts suggests that the supported bimetallic nanoparticle structure may be similar to the Pt-terminated configurations identified in theoretical calculations and surface science. The current work demonstrates a direct link between model surfaces and supported catalysts, providing a promising and efficient way to design efficient hydrogenation bimetallic catalysts.

Acknowledgements

This work was supported by the United States Department of Energy, Office of Basic Energy Sciences (DE-FG02-00ER15104). The authors from the Peking University acknowledge support from the Major State Basic Research Development Program (Grant No. 2011CB808702) and the China Scholarship Council. The authors would like to thank William Lonergan for assistance with batch reactor studies and Weiting Yu for DFT calculations.

References

1 J. H. Sinfelt, *Acc. Chem. Res.*, 1977, **10**, 15–20.
2 J. P. Breen, R. Burch, K. Griffin, C. Hardacre, M. Hayes, X. Huang and S. D. O'Brien, *J. Catal.*, 2005, **236**, 270–281.
3 E. P. Maris, W. C. Ketchie, M. Murayama and R. J. Davis, *J. Catal.*, 2007, **251**, 281–294.
4 J. G. Chen, C. A. Menning and M. B. Zellner, *Surf. Sci. Rep.*, 2008, **63**, 201–254.
5 B. Hammer and J. K. Norskov, *Surf. Sci.*, 1995, **343**, 211–220.
6 J. A. Rodriguez, *Surf. Sci. Rep.*, 1996, **24**, 223–287.
7 M. P. Humbert and J. G. Chen, *J. Catal.*, 2008, **257**, 297–306.
8 D. A. Hansgen, D. G. Vlachos and J. G. Chen, *Nat. Chem.*, 2010, **2**, 484–489.
9 S. L. Lu, W. W. Lonergan, J. P. Bosco, S. R. Wang, Y. X. Zhu, Y. C. Xie and J. G. Chen, *J. Catal.*, 2008, **259**, 260–268.
10 J. G. Chen, S. T. Qi, M. P. Humbert, C. A. Menning and Y. X. Zhu, *Acta Phys. -Chim. Sin.*, 2010, **26**, 869–876.
11 W. W. Lonergan, D. G. Vlachos and J. G. Chen, *J. Catal.*, 2010, **271**, 239–250.
12 S. Nishimura, *Handbook of Heterogeneous Catalytic Hydrogenation for Organic Synthesis*, Wiley, New York, 2001, pp. 170–199.
13 P. Maki-Arvela, J. Hajek, T. Salmi and D. Y. Murzin, *Appl. Catal., A*, 2005, **292**, 1–49.
14 G. M. R. van Druten, L. Aksu and V. Ponec, *Appl. Catal., A*, 1997, **149**, 181–187.
15 G. M. R. van Druten and V. Ponec, *React. Kinet. Catal. Lett.*, 1999, **68**, 15–23.
16 G. M. R. van Druten and V. Ponec, *Appl. Catal., A*, 2000, **191**, 153–162.
17 X. Q. Wang, R. Y. Saleh and U. S. Ozkan, *J. Catal.*, 2005, **231**, 20–32.
18 D. Loffreda, F. Delbecq, F. Vigne and P. Sautet, *J. Am. Chem. Soc.*, 2006, **128**, 1316–1323.
19 L. E. Murillo, A. M. Goda and J. G. Chen, *J. Am. Chem. Soc.*, 2007, **129**, 7101–7105.
20 K. H. Lim, A. B. Mohammad, I. V. Yudanov, K. M. Neyman, M. Bron, P. Claus and N. Rosch, *J. Phys. Chem. C*, 2009, **113**, 13231–13240.
21 N. Ji, T. Zhang, M. Y. Zheng, A. Q. Wang, H. Wang, X. D. Wang and J. G. Chen, *Angew. Chem., Int. Ed.*, 2008, **47**, 8510–8513.
22 X. L. Zhu, L. L. Lobban, R. G. Mallinson and D. E. Resasco, *J. Catal.*, 2010, **271**, 88–98.
23 G. Kresse and J. Hafner, *Phys. Rev. B: Condens. Matter*, 1993, **47**, 558–561.
24 G. Kresse and J. Furthmuller, *Phys. Rev. B: Condens. Matter*, 1996, **54**, 11169–11186.
25 R. Alcala, J. Greeley, M. Mavrikakis and J. A. Dumesic, *J. Chem. Phys.*, 2002, **116**, 8973–8980.
26 A. L. Stottlemyer, H. Ren and J. G. Chen, *Surf. Sci.*, 2009, **603**, 2630–2638.
27 C. A. Menning and J. G. Chen, *J. Chem. Phys.*, 2008, **128**, 164703.
28 P. Basu, T. H. Ballinger and J. T. Yates, *Rev. Sci. Instrum.*, 1988, **59**, 1321–1327.
29 N. McMillan, C. Snively and J. Lauterbach, *Surf. Sci.*, 2007, **601**, 772–780.
30 NIST Chemistry WebBook, National Institute of Standards and Technology, http://webbook.nist.gov/.
31 S. R. Wang, W. Lin, Y. X. Zhu, Y. C. Xie and J. G. Chen, *Chin. J. Catal.*, 2006, **27**, 301–303.
32 C. A. Menning and J. G. Chen, *J. Chem. Phys.*, 2009, **130**, 174709.
33 C. A. Menning and J. G. Chen, *J. Power Sources*, 2010, **195**, 3140–3144.